

# Enumeration of many-body skeleton diagrams

Luca Guido Molinari<sup>1,2</sup> and Nicola Manini<sup>1,3</sup>

<sup>1</sup>*Dipartimento di Fisica dell'Università degli Studi di Milano, Via Celoria 16, I-20133 Milano and European Theoretical Spectroscopy Facility (E.T.S.F.)*

<sup>2</sup>*I.N.F.N. Sezione di Milano*

<sup>3</sup>*INFM-CNR, Unità di Milano, Milano, Italy*

(Dated: February 2, 2008)

The many-body dynamics of interacting electrons in condensed matter and quantum chemistry is often studied at the quasiparticle level, where the perturbative diagrammatic series is partially resummed. Based on Hedin's equations for self-energy, polarization, propagator, effective potential, and vertex function in zero dimension of space-time, dressed Feynman (skeleton) diagrams are enumerated. Such diagram counts provide useful basic checks for extensions of the theory for future realistic simulations.

PACS numbers: 71.10.-w, 24.10.Cn, 11.10.Gh

## I. INTRODUCTION

Current research in electronic properties of molecules, nanocomponents, and solids has gone far beyond the mean-field density-functional description. Many-body methods are employed routinely, at the level of quasiparticles, to describe excitations accurately<sup>1,2,3</sup>. Propagators and interactions are renormalized to obtain an effective theory of weakly interacting quasiparticles. This is achieved by infinite resummations of Feynman diagrams, that are brought to a smaller class of skeleton diagrams<sup>4</sup>. The reduction in number should correspond to better analytic behavior in space-time of the individual dressed diagrams, as it occurs in random-phase or ladder resummations<sup>5</sup>.

In this report, we show how skeleton Feynman diagrams of various types can be enumerated for the exact many-body theory and its GW approximation<sup>1,2,3</sup>. We take as our starting point the standard formulation of the many-body problem of  $N$  interacting fermions provided by the set of five Hedin's equations<sup>2,3,6,7</sup> for the propagator  $G(1, 2)$ , effective potential  $W(1, 2)$ , irreducible self-energy  $\Sigma(1, 2)$ , irreducible polarization  $\Pi(1, 2)$ , and irreducible vertex  $\Gamma(1; 2, 3)$ .

In zero dimension of space *and* time, the combinatorial content of Wick's expansion survives, producing the same Feynman diagrams in the perturbative expansion of the correlators as in conventional 3+1 dimensions. These correlators no longer carry space-time labels, and

do not correspond to space-time functions. However, they continue to solve Hedin's equations, which can indeed be derived from considerations about the topology of diagrams<sup>4</sup>. In zero dimensions ( $d = 0$ ), four of Hedin's equations become algebraic, in terms of the scalar variables  $g$  and  $v$ , representing the Hartree propagator (computed with the exact density provided by  $G$ ) and the bare interparticle interaction respectively. The functional derivative in the equation for the vertex becomes an ordinary derivative. The five equations read:

$$G = g + g\Sigma G, \quad W = v + v\Pi W, \quad (1)$$

$$\Sigma = iGW\Gamma, \quad \Pi = i\ell G^2\Gamma, \quad (2)$$

$$\Gamma = 1 + \Gamma G^2 \frac{\partial \Sigma}{\partial G}. \quad (3)$$

The parameter  $\ell$  is introduced to count fermion loops: in Hedin's equations for the electron,  $\ell = -2$  because of spin degeneracy and Feynman's rule for the fermionic loop. The diagrammatic meaning of Hedin's equations is simple: Eqs. (1) correspond to Dyson's equations that define the proper self-energy and polarization insertions for the propagator and the effective potential, Eqs. (2) translate the unique skeleton structure<sup>5</sup> of  $\Sigma$  and  $\Pi$ , shown in Fig. 1. Finally, the vertex equation (3) shows that vertex diagrams arise from self-energy diagrams, by "pinching" a  $G$  line with a vertex (remove a line  $G$  and replace it with  $G\Gamma G$ ): this follows from the functional definition of the vertex<sup>6,8,9</sup>. In the GW approximation all corrections to the bare vertex are neglected: the approximation  $\Gamma = 1$  replaces the exact vertex equation (3).

## II. ENUMERATION OF FEYNMAN DIAGRAMS

The perturbative solution of Hedin's equations in zero dimension provides numerical coefficients which enumerate the Feynman diagrams for the five correlators involved. The ordinary perturbation expansion is carried out in the bare parameters  $v$  and  $g$ . However, it is often convenient to expand in different "renormalized" variables, such as  $v$  and  $G$ , or  $W$  and  $G$ , or  $G, W$  and  $\Gamma$ . These

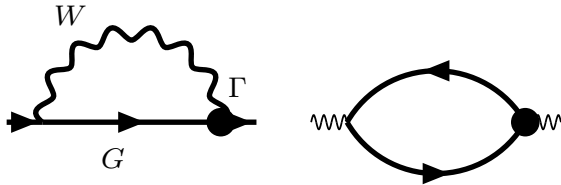


FIG. 1: The unique fully dressed skeleton diagrams for self-energy (left) and polarization (right).

TABLE I: The number of  $n^{\text{th}}$ -order skeleton diagrams for the vertex function in the five renormalization schemes considered in the text.

$n$	1	2	3	4	5	6	7	8	9	10
$\Gamma(x)$	1	9	100	1323	20088	342430	6461208	133618275	3006094768	73139285178
$\Gamma(y)$	1	7	63	729	10113	161935	2923135	58547761	1286468225	30747331223
$\Gamma(t)$	1	6	52	602	8223	128917	2273716	44509914	957408649	22449011336
$\Gamma(z)$	1	6	49	542	7278	113824	2017881	39842934	865391422	20486717908
$\Gamma(u)$	1	3	13	147	1965	30979	559357	11289219	250794109	6066778627

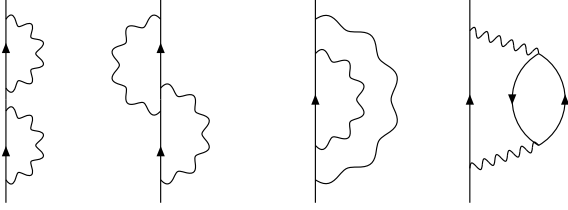


FIG. 2: The four diagrams for  $G$  at second order in  $x$ .

expansions count Feynman diagrams where, respectively, the propagator or both the propagator and the potential, or also the vertex, have been fully renormalized. Such diagrams where self-energy contributions of various types are resummed, are called *skeleton* graphs<sup>4,5</sup>. Different levels of resummations will be considered below, including a renormalization based on GW correlators.

#### A. $x = g^2v$ -expansion

Standard perturbation theory in the bare interaction  $v$  has been studied in  $d = 0$  by various authors<sup>10,11</sup> by considering the path integral formulation of the interacting field, which degenerates to an ordinary integral. An approach based on Hedin's equations is very convenient to deal with the Hartree propagator  $g$  in place of the bare one, and explicit counting numbers can be obtained<sup>9</sup>.

Here, the natural dimensionless expansion parameter is  $x = ig^2v$ . As an example, we provide the equation for  $Z(x) = G/g$ , where  $Z$  is the renormalization factor due to self-energy corrections. The algebraic equations (1,2) yield

$$\ell x Z^2(x) \Gamma(x) = 1 - \frac{1}{1 - \ell + \ell Z(x)}. \quad (4)$$

The GW approximation ( $\Gamma = 1$ ), generates a cubic equation for  $Z_{GW}$ . For the complete theory, we rewrite the vertex equation (3), in a form<sup>9</sup> where  $G$  is traded for  $g$ :

$$\Gamma(x) = 1 + g^2 \frac{\partial \Sigma}{\partial g} = \frac{1}{Z(x)} - 2x \frac{d}{dx} \frac{1}{Z(x)}. \quad (5)$$

Equations (4) and (5) combine to a closed equation for  $Z$ :

$$2\ell x^2 \frac{dZ}{dx} = 1 - \ell x Z(x) - \frac{1}{1 - \ell + \ell Z(x)}, \quad (6)$$

with the initial condition  $Z(0) = 1$ . The solution as a series expansion in  $x$  provides the number of Feynman diagrams that contribute to each order to the propagator  $G$

$$Z(x) = 1 + x + (3 + \ell)x^2 + (15 + 11\ell + \ell^2)x^3 + \dots \quad (7)$$

The  $\ell$  powers represent the loop contents. For example, at second order in  $x$ , the theory involves 3 diagrams with no loops, and 1 diagram with one loop; they are shown in Fig. 2. By substituting the power series for  $Z(x)$  into Eq. (5), we obtain the diagram count for the vertex function:

$$\Gamma(x) = 1 + x + 3(2 + \ell)x^2 + 5(10 + 9\ell + \ell^2)x^3 + \dots \quad (8)$$

Table I reports the total number of vertex diagrams up to 10<sup>th</sup> order, obtained by taking  $\ell = 1$  in the expansion for  $\Gamma(x)$ .

#### B. $y = G^2v$ -skeleton expansion

When all self-energy insertions of the propagator are resummed, one ends up with Feynman diagrams where

the propagator lines correspond to the exact  $G$ , while the interaction lines continue to correspond to the bare  $v$ . This resummation is obtained by using the expansion parameter  $y = iG^2v$ . It is possible to obtain a closed

equation for the vertex function. First write the self-energy as

$$\Sigma = iGWT = iG \frac{v}{1 - v\Pi} \Gamma = \frac{1}{G} \frac{y\Gamma}{1 - y\ell\Gamma}. \quad (9)$$

Next evaluate the vertex function in Eq. (3) by means of Eq. (9), and obtain a differential equation for  $\Gamma(y)$ :

$$2y^2\Gamma \frac{d\Gamma}{dy} = -1 + (1 + 2y\ell)\Gamma - y\Gamma^2(1 + 2\ell + y\ell^2) + y^2\Gamma^3\ell(\ell - 1). \quad (10)$$

This equation must be solved with the initial condition  $\Gamma(0) = 1$ . The series expansion of the solution counts skeleton vertex diagrams with dressed propagators and bare interactions:

$$\Gamma(y) = 1 + y + (4 + 3\ell)y^2 + (27 + 31\ell + 5\ell^2)y^3 + \dots \quad (11)$$

Table I lists the total number of these diagrams up to order  $n = 10$ , by taking  $\ell = 1$  in the expansion for  $\Gamma(y)$ , as was done above.

The enumeration of skeleton diagrams of the polarization  $\Pi = i\ell G^2\Gamma(y)$  coincides with that of  $\Gamma(y)$ . The skeleton expansion of  $\Sigma$  results from Eq. (9):

$$\Sigma/iGv = 1 + (1 + \ell)y + (4 + 5\ell + \ell^2)y^2 + (27 + 40\ell + 14\ell^2 + \ell^3)y^3 + \dots \quad (12)$$

In the expansion in terms of the bare parameter  $x$ ,  $\Pi$  and  $\Sigma$  shared the diagram counting,<sup>9</sup> while this property does not apply to the  $y$  expansion at hand.

The  $G^2v$ -expansion of  $\Sigma$  is interesting for the theory of the Luttinger-Ward  $\Phi$ -functional<sup>12,13</sup>. By closing all  $\Sigma[G, v]$  skeleton graphs with a  $G$  line, and dividing each one by the number of  $G$  lines it contains, one obtains a functional with the property of yielding the self-energy and the reducible polarization:

$$\Sigma(1, 2) = \frac{\delta\Phi[G, v]}{\delta G(2, 1)}, \quad \tilde{\Pi}(1, 2) = -2 \frac{\delta\Phi[G, v]}{\delta v(2, 1)}. \quad (13)$$

In  $d = 0$ , the functional  $\Phi[G, v]$  turns into an ordinary function of  $y = iG^2v$ .

$$\begin{aligned} \Phi(y) &= \frac{1}{2} \int_0^y dy' \frac{\Gamma(y')}{1 - \ell y' \Gamma(y')} \\ &= \frac{y}{2} + (1 + \ell) \frac{y^2}{4} + (4 + 4\ell + \ell^2) \frac{y^3}{6} + \dots \end{aligned} \quad (14)$$

This last expression provides the appropriate diagram counting and fractional weights for  $\Phi(y)$  in any dimension.

### C. $z = G^2W$ -skeleton expansion

Resummation of both self-energy and polarization insertions leads to skeleton diagrams with exact propagators  $G$  and interactions  $W$ . Here, the natural expansion

parameter is  $z = iG^2W$ . The parameter  $z$  is linked as follows

$$z = iG^2 \frac{v}{1 - i\ell v \Gamma G^2} = \frac{y}{1 - \ell y \Gamma} \quad (15)$$

to the parameter  $y = iG^2v$  of the previous expansion (11). Inversion yields  $y = z[1 + \ell z\Gamma(z)]^{-1}$ . By entering this relation into the differential equation (10) for  $\Gamma(y)$ , which is now viewed as a function of  $z$ , we obtain

$$z^2 \frac{d\Gamma(z)}{dz} = \frac{1 - \Gamma(z) + z\Gamma^2(z) + 2\ell z^2\Gamma^3(z)}{\ell - (2 + \ell)\Gamma(z) - 3\ell z\Gamma^2(z)}. \quad (16)$$

The appropriate series expansion counts  $G^2W$ -dressed vertex diagrams:

$$\Gamma(z) = 1 + z + 2(2 + \ell)z^2 + (27 + 22\ell)z^3 + \dots \quad (17)$$

Table I lists the total number of these  $\Gamma(z)$  diagrams up to order  $n = 10$ . Both  $\Sigma = iGWT(z)$  and  $\Pi = i\ell G^2\Gamma(z)$  have the same total  $G^2W$ -counting numbers as the vertex.

In the  $G^2W$ -expansion, it is natural to define<sup>12</sup> the functional  $\Psi[G, W]$ , which generalizes Eq. (13) and generates the self-energy and the irreducible polarization as follows:

$$\Sigma(1, 2) = \frac{\delta\Psi[G, W]}{\delta G(2, 1)}, \quad \Pi(1, 2) = -2 \frac{\delta\Psi[G, W]}{\delta W(2, 1)}. \quad (18)$$

The diagrammatic construction of  $\Psi$  is the same as for  $\Phi$ : close the skeleton graphs of  $\Sigma = iGWT[G, W]$  with a  $G$  line and divide by the number of  $G$  lines that the graph contains. In  $d = 0$  we have  $G\Sigma = z\Gamma(z)$ ; to divide by the number of  $G$  lines that each  $G\Sigma$ -diagram contains, corresponds to the integral

$$\Psi(z) = \frac{1}{2} \int_0^z dz' \Gamma(z') = \frac{z}{2} + \frac{z^2}{4} + (2 + \ell) \frac{z^3}{3} + \dots \quad (19)$$

### D. $u = G^2WT^2$ -skeleton expansion

The  $G^2W$ -expansion resums all self-energy and polarization insertions, and skeleton diagrams of various order in  $z$  result just because of vertex contributions. If vertex diagrams are summed as well, each of the self-energy and the polarization is brought to a unique skeleton diagram depicted in Fig. 1. Vertex diagrams cannot be brought to a finite collection of skeleton diagrams. We may nevertheless resum vertex insertions in all vertex diagrams, and enumerate the resulting vertex skeleton diagrams, where all lines and vertices are resummed.

This is achieved by noting that in a vertex diagram, each  $W$  line ends in two vertices. However, the vertex which the Coulomb external line is attached to, is left out (see Fig. 3 for some vertex diagrams). We then write  $\Gamma = 1 + \Gamma\gamma(u)$ , in terms of the expansion variable  $u = iG^2WT^2 = z\Gamma^2(z)$ . The factor  $\Gamma$  in front of  $\gamma(u)$  accounts for the left-out vertex.

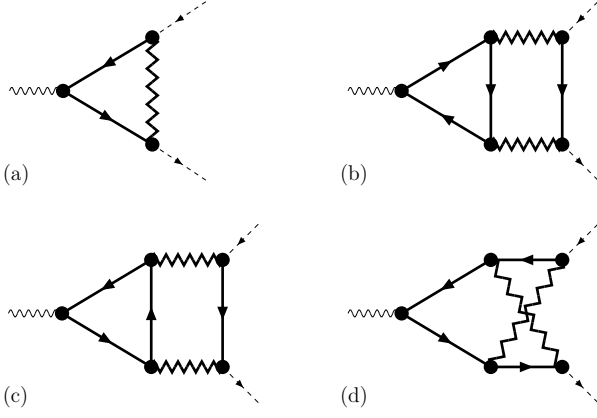


FIG. 3: All first-order (a) and second-order (b,c,d) vertex diagrams in  $u$  expansion.

The Taylor expansion of  $\gamma(u)$  enumerates all dressed fully renormalized vertex diagrams. An equation for  $\gamma$  is obtained from the relation

$$\frac{d\gamma}{du} = \frac{dz}{du} \frac{d}{dz} \frac{\Gamma - 1}{\Gamma} = \frac{1}{\Gamma^2} \frac{d\Gamma/dz}{\Gamma^2 + 2z\Gamma d\Gamma/dz}, \quad (20)$$

where we enter  $d\Gamma/dz$  given by Eq. (16):

$$u \frac{d\gamma}{du} = (1 - \gamma) \frac{2\ell u^2(1 - \gamma)^2 + u(1 - \gamma) - \gamma}{\ell u^2(1 - \gamma)^2 - \ell u\gamma(1 - \gamma) - 2\gamma}. \quad (21)$$

This equation is solved with initial condition  $\gamma(0) = 0$ . The resulting  $u$ -expansion for  $\Gamma$  is

$$\begin{aligned} \Gamma(u) = & 1 + (\Gamma u) + (1 + 2\ell)(\Gamma u^2) + (7 + 6\ell)(\Gamma u^3) \\ & + (63 + 74\ell + 10\ell^2)(\Gamma u^4) + \dots \end{aligned} \quad (22)$$

The diagrams of first and second order are shown in Fig. 3 (the next 13 third-order diagrams coincide with those of QED, drawn in Ref. 10). This  $u$ -expansion represents the “ultimate” skeleton expansion, where all ingredients of Hedin’s equations have been renormalized. Indeed, as apparent in Table I, the diagram count is smallest in the  $u$  expansion at hand.

### E. $t = (G^2W)_{GW}$ -skeleton expansion

In the GW approximation ( $\Gamma = 1$ ), in physical dimensions, Hedin’s equations are a system of ordinary integral equations for  $G_{GW}$ ,  $\Sigma_{GW}$ ,  $W_{GW}$  and  $\Pi_{GW}$ . It is conceivable that in a near future increased computer power will allow us to solve these equations in fully self-consistent GW: this would make the GW approximation the zeroth-order stage of a subsequent attack of the full many-body problem, where vertex corrections are included perturbatively. The problem of including vertex corrections

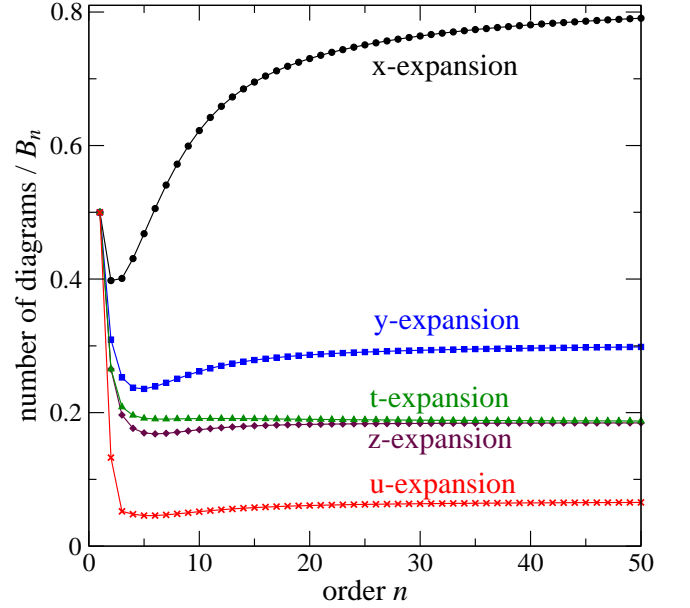


FIG. 4: (color online) Number of vertex diagrams at order  $n$ , divided by the asymptotic expression  $B_n$  defined in Eq. (27), for the different renormalization schemes realized in Sec. II A [ $x$  – Eq. (7)], Sec. II B [ $y$  – Eq. (11)], Sec. II E [ $t$  – Eq. (26)], Sec. II C [ $z$  – Eq. (17)], and Sec. II D [ $u$  – Eq. (22)].

in a systematic way is an important target of present-day research, to overcome several limitations of the non-conservative GW<sup>1,14,15</sup>. It is therefore of interest to count the diagrams where  $g$  and  $v$  lines are dressed (resummed) to include all their GW self-energy and polarization insertions.

The counting problem is solved in  $d = 0$  by considering the expansion parameter  $t = iG_{GW}^2 W_{GW}$ . With simple algebra, the following two equations for the vertex and the ratio  $Z_{GW}(t) = G/G_{GW}$  are obtained:

$$tZ_{GW}^2(t)\Gamma(t) = \frac{[(1+t)Z_{GW}(t) - 1](1 + \ell t)}{1 - \ell + \ell(1+t)Z_{GW}(t)}, \quad (23)$$

$$\begin{aligned} 2t^2 \frac{dZ_{GW}}{dt} = & (1 - t - 2\ell t^2) \frac{(1+t)Z_{GW}(t) - 1}{1 - \ell + \ell(1+t)Z_{GW}(t)} \\ & - \frac{t}{1 + \ell t} Z_{GW}(t). \end{aligned} \quad (24)$$

The perturbative solutions are:

$$Z_{GW}(t) = 1 + t^2 + (5 + 3\ell)t^3 + \dots \quad (25)$$

$$\Gamma(t) = 1 + t + 2(2 + \ell)t^2 + (29 + 23\ell)t^3 + \dots \quad (26)$$

Table I lists the total number of these  $\Gamma(t)$  diagrams up to order  $n = 10$ .

## III. ASYMPTOTICS

To estimate asymptotic behaviors is not simple in the present approach. However, the topology of many-body

diagrams with two-body interaction is the same as in relativistic quantum electrodynamics (QED), with a difference: because of exact particle-antiparticle symmetry, QED diagrams with loops involving an odd number of fermion lines cancel (Furry's theorem<sup>8</sup>). Therefore, many-body skeleton diagrams grow faster in number than QED ones.

The functional approach, in the saddle point expansion, is better suited for asymptotics. This problem in physical dimensions has been studied for QED by several authors, based on Lipatov's powerful method<sup>16,17</sup>. From the tabulated QED asymptotic values<sup>10</sup> in  $d = 0$ , one can infer the leading behavior of many-body vertex skeleton diagrams. Consider the series for the vertex  $\Gamma(\theta) = \sum_n A_n \theta^n$ , in one of the renormalization schemes ( $\theta = x, y, z, t, u$ ) outlined above. We obtain

$$A_n = B_n (c_0 + c_1/n + \dots), \quad B_n = n! 2^n n^{3/2}. \quad (27)$$

In Fig. 4 the asymptotic behavior is checked on the first 50 coefficients of the five different vertex skeleton expansions computed in the present work. Indeed, in all expansions, whether bare or renormalized, the number of vertex diagrams grows with the order  $n$  roughly as  $B_n$ , thus leading to divergent power series, like in QED. The renormalization scheme only affects the subleading coefficients  $c_i$ . As expected, the “ultimate”  $u$  expansion, involving wider diagram resummations leads to fewer dia-

grams than all other “less renormalized” expansions. For large  $n$ , the diagram count is essentially the same for the  $z$  expansion, including renormalization to both the propagator and the interaction, and for the  $t$  expansion around Hedin's GW approximation.

#### IV. CONCLUSIONS

The present method for enumerating skeleton diagrams is based on Hedin's equations and it is very efficient. Simple changes of the expansion variable produce various renormalizations schemes, in the form of differential equations that can easily be solved by series. The coefficients of these series are integers that count skeleton diagrams. These are useful as a check for any diagrammatic approach to the many-body problem in realistic dimensions. As expected, the number of diagrams, whether renormalized or not, grows factorially with the order.

#### Acknowledgments

This work was funded in part by the EU's 6th Framework Programme through the NANOQUANTA Network of Excellence (NMP4-CT-2004-500198)

- 
- <sup>1</sup> G. Onida, L. Reining, and A. Rubio, *Rev. Mod. Phys.* **74**, 601 (2002).
  - <sup>2</sup> W. G. Aulbur, L. Jönsson, and J. W. Wilkins, *Solid State Physics* **54**, p. 1, edited by H. Ehrenreich and F. Spaepen (Academic, New York, 2000).
  - <sup>3</sup> F. Aryasetiawan and O. Gunnarsson, *Rep. Progr. Phys.* **61**, 237 (1998).
  - <sup>4</sup> J. D. Bjorken and S. D. Drell, *Relativistic Quantum Fields*, (McGraw Hill, New York, 1965).
  - <sup>5</sup> A. L. Fetter, J. D. Walecka, *Quantum Theory of Many-Particle Systems*, (McGraw-Hill, New York, 1971).
  - <sup>6</sup> L. Hedin, *Phys. Rev.* **139**, A796 (1965).
  - <sup>7</sup> L. Hedin and S. Lundqvist, *Solid State Physics* **23**, p. 1, edited by F. Seitz, D. Turnbull, and H. Ehrenreich (Academic, New York, 1969).
  - <sup>8</sup> C. Itzykson and J. P. Zuber, *Quantum Field Theory*, (McGraw Hill, New York, 1980).
  - <sup>9</sup> L. Molinari, *Phys. Rev. B* **71**, 113102 (2005).
  - <sup>10</sup> P. Cvitanovic, B. Lautrup, and R. B. Pearson, *Phys. Rev. D* **18**, 1939 (1978).
  - <sup>11</sup> E. N. Argyres, A. F. W. van Hameren, R. H. P. Kleiss, and C. G. Papadopoulos, *Eur. Phys. J. C* **19**, 567 (2001).
  - <sup>12</sup> C.-O. Almbladh, U. Von Barth, and R. Van Leeuwen, *Variational total energies from  $\Phi$ - and  $\Psi$ -derivable theories*, *Int. J. Mod. Phys. B* **13**, 535 (1999).
  - <sup>13</sup> G. F. Giuliani and G. Vignale, *Quantum Theory of the Electron Liquid*, (Cambridge University Press, 2005).
  - <sup>14</sup> A. Schindlmayr and R. W. Godby, *Phys. Rev. Lett.* **80**, 1702 (1998).
  - <sup>15</sup> F. Bruneval, F. Sottile, V. Olevano, R. Del Sole, and L. Reining, *Phys. Rev. Lett.* **94**, 186402 (2005).
  - <sup>16</sup> C. Itzykson, G. Parisi, and J. B. Zuber, *Phys. Rev. D* **16**, 996 (1977).
  - <sup>17</sup> I. M. Suslov, *Divergent Perturbation Series*, *Zh. Eksp. Teor. Fiz.* **127**, 1350 (2005); *Sov. Phys. JETP* **100**, 1188 (2005); hep-th/0510142.